

Selective Equilibration of Spin-Polarized Quantum Hall Edge States in Graphene

F. Amet,¹ J. R. Williams,² K. Watanabe,³ T. Taniguchi,³ and D. Goldhaber-Gordon²

¹*Department of Applied Physics, Stanford University, Stanford, California 94305, USA*

²*Department of Physics, Stanford University, Stanford, California 94305, USA*

³*Advanced Materials Laboratory, National Institute for Materials Science, 1-1 Namiki, Tsukuba 305-0044, Japan*

(Received 3 July 2013; revised manuscript received 25 November 2013; published 12 May 2014)

We report on transport measurements of dual-gated, single-layer graphene devices in the quantum Hall regime, allowing for independent control of the filling factors in adjoining regions. Progress in device quality allows us to study scattering between edge states when the fourfold degeneracy of the Landau level is lifted by electron correlations, causing edge states to be spin and/or valley polarized. In this new regime, we observe a dramatic departure from the equilibration seen in more disordered devices: edge states with opposite spins propagate without mixing. As a result, the degree of equilibration inferred from transport can reveal the spin polarization of the ground state at each filling factor. In particular, the first Landau level is shown to be spin polarized at half filling, providing an independent confirmation of a conclusion of Young *et al.* [Nat. Phys. **8**, 550 (2012)]. The conductance in the bipolar regime is strongly suppressed, indicating that copropagating edge states, even with the same spin, do not equilibrate along *PN* interfaces. We attribute this behavior to the formation of an insulating $\nu = 0$ stripe at the *PN* interface.

DOI: 10.1103/PhysRevLett.112.196601

PACS numbers: 72.80.Vp, 73.43.-f

At low magnetic fields, the electronic properties of graphene are well described by a noninteracting Dirac Hamiltonian [1,2], with fourfold degeneracy associated with spin and valley isospin, an additional degree of freedom due to the hexagonal crystal lattice of graphene. As a result, graphene exhibits an anomalous quantum Hall effect with a transverse conductance quantized as $4(n + \frac{1}{2})e^2/h$, where n is an integer [3–5]. At higher fields, Zeeman coupling and electron correlations can lift the fourfold degeneracy of the energy spectrum, resulting in spin- and valley-polarized Landau levels [6]. The nature of the ground state for each Landau level at partial filling depends on which symmetry-breaking energy dominates, a controversial topic over the years [6–19]. While progress has been made in our understanding of the symmetry-breaking of partially filled Landau levels, direct observation of their polarization remains difficult. Previous work focused on the in-plane and perpendicular field dependence of the bulk 2D quantum Hall gaps [7,19,30], but an alternative approach would be to directly study edge transport.

To this end, we measured the conductance of eight dual-gated graphene devices in the quantum Hall regime, at temperature $T = 250$ mK and for magnetic field B up to 14 T. Our samples use a hexagonal boron-nitride substrate (*h*-BN), which greatly improves the electronic performance of graphene devices [20], and a suspended top gate (TG) [21–23]. The resulting quality of our devices allows us to study bipolar transport where the spin and valley fourfold degeneracies of the Landau levels are fully lifted. When the filling factors under and outside the top gate differ, the two-terminal conductance of such devices strongly depends on scattering between edge states, with

new plateaus resulting from their mixing. The values of these plateaus suggest that edge states with different spin polarization do not equilibrate at the scale of our devices. This contrasts with the valley polarization, since inter-valley scattering along the disordered edges of these samples causes edge states with different valley polarization—but same spin—to equilibrate. The pattern of equilibration for each pair of filling factors depends on the ground states at quarter and half filling for the zeroth and first Landau levels. In particular, our measured conductance plateaus at filling factor $\nu = 4$ are consistent with a spin-polarized first Landau level at half filling. The conductance in the bipolar regime becomes vanishingly small as B increases, contrary to previous observations [22,26,27], suggesting the formation of a narrow $\nu = 0$ insulating stripe along the *PN* interface.

Here, we present a unified data set from a single device, called device A; additional data from similar devices are available in Ref. [24]. Device A is a 3 μm long, 1 μm wide graphene stripe, with a metallic top-gate suspended ~ 90 nm above the middle third of the device [Fig. 1(d)]. Details of the fabrication are described in Ref. [21,24]. The two-terminal conductance g is measured in a ³He cryostat using a conventional lock-in setup with a 100 μV voltage-bias excitation at 137 Hz. Resistance $R \equiv 1/g$ at $B = 0$ as a function of the back-gate (BG) voltage V_{BG} shows residual doping $\delta n \sim 10^{11} \text{ cm}^{-2}$, peak resistance 30 k Ω and mobility 120000 cm^2/Vs at $T = 2$ K [Fig. 1(e)], demonstrating the high quality of this sample. $R(V_{\text{TG}})$ shows the usual electron-hole asymmetry characteristic of graphene *PN* junctions. The back-gate capacitance extracted from magneto-transport measurements is $5.9 \times 10^{10} \text{ cm}^{-2}/\text{V}$,

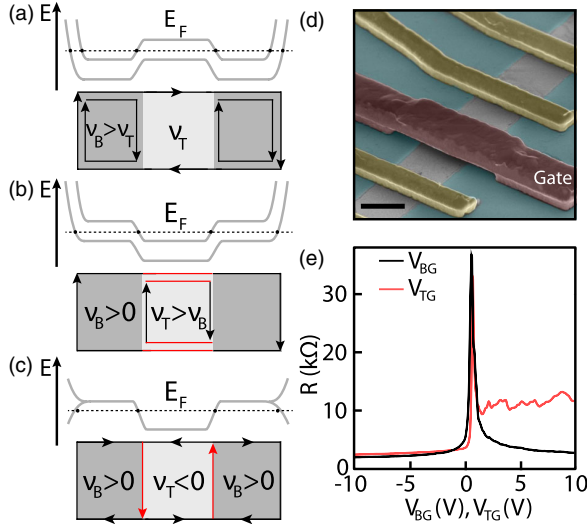


FIG. 1 (color online). (a) Spatial variations of Landau levels in the case $\nu_B > \nu_T > 0$: levels are bent by the confinement potential close to the edges of the device. Only ν_T edge states are fully transmitted through the barrier. (b) Landau levels in the case $\nu_T > \nu_B > 0$. Equilibration occurs along the physical edges of the flake under the top gate (stretch of edge shown in red). (c) Landau levels in the case $\nu_T \nu_B < 0$, with a degenerate zeroth level. This degeneracy is lifted close to the edges. Equilibration may occur along the PN interface (red). (d) False-colored electron micrograph of a top-gated device: the top gate (purple) is suspended above the graphene flake (gray). The whole device rests on a boron-nitride substrate (blue). The scale bar is $1 \mu\text{m}$. (e) Resistance R as a function of V_{BG} and V_{TG} , measured at a temperature $T = 2 \text{ K}$.

and the top-to-back-gate capacitance ratio is 1.05, in good agreement with the geometry of the device as described in Ref. [24].

In the quantum Hall regime, the conductance depends on the filling factors under and outside the top-gated region, ν_T and ν_B , respectively. When ν_T is reduced below ν_B , only ν_T edge states are fully transmitted through the top-gated region [Fig. 1(a)], while the others are fully reflected, allowing control of the edge states' trajectories. Two other regimes are of particular interest because the overall two-terminal conductance g strongly depends on the interactions between edge states [25]. In the unipolar regime, if $|\nu_T| > |\nu_B|$ the conductance depends on scattering between edge states under the gate. When Landau levels are degenerate, the conductance has been observed to be reduced from $\nu_B e^2/h$ and quantized as $g_{\nu_T, \nu_B} = \nu_T \nu_B / (2\nu_T - \nu_B)$ [22,26,27]. This was attributed in Ref. [25] to the complete mixing of edge states: charge carriers are randomly scattered between edge states and have a probability $1/\nu_T$ to be ejected in any given edge state after propagating under the gate, regardless of the state into which they were injected at the contacts [25]. When the spin and valley degeneracies are lifted, however, it is not clear whether this model still applies since scattering

between edge states might depend on their spin and/or valley polarization. In the bipolar regime, the role of scattering is even starker: edge states in the electron- and hole-doped regions have opposite chirality, so g is nonzero only if these equilibrate while copropagating along the PN interfaces [Fig. 1(c)]. Previous work showed that for dual-gated devices on a SiO_2 substrate, scattering along the PN interface is strong enough to completely mix edge states in this regime as well, resulting in new conductance plateaus at fractional multiples of the quantum of conductance e^2/h [22,26,27].

A map of $g(V_{TG}, V_{BG})$ is shown at $B = 14 \text{ T}$, $T = 1 \text{ K}$ on Fig. 2(a). At this field, electron interactions are strong enough to fully lift the spin and valley degeneracy of the Landau levels [6–9,11–19]. As a result, when tuning ν_T from -6 to 0 at constant $\nu_B = -6$, g shows plateaus at every multiple of e^2/h as fewer and fewer edge states are transmitted through the potential barrier [Fig. 2(b)]. These edge

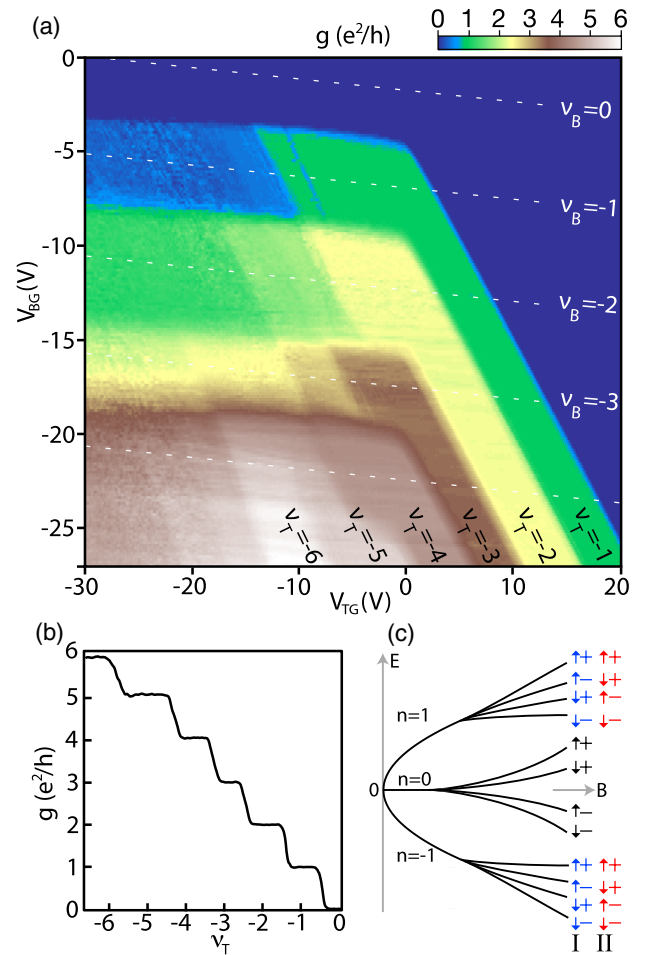


FIG. 2 (color online). (a) Two-terminal conductance g as a function of both gate voltages V_{TG} and V_{BG} , measured at 14 T , $T = 1 \text{ K}$. (b) Partial transmission of edge states at $\nu_B = -6$ as the filling factor under the top gate is depleted. (c) Energy diagram for spin- (I) or valley-polarized (II) first Landau level at half-filling.

states can *a priori* be spin- and/or valley-polarized, depending on the ground state in the bulk for each filling factor. It was pointed out in Ref. [28] that the valley degeneracy of the zeroth Landau level is lifted by the confinement potential at the edges. As a result, the existence or lack of counter-propagating spin-polarized edge states at $\nu = 0$ depends on the competition between Zeeman coupling and valley symmetry breaking interactions in the half-filled zeroth Landau level [11,18,28,29]. For filling factors $\nu = 1$ and $\nu = 2$, the edge states share a common valley polarization—which may correspond to a superposition of the K and K' valleys, determined by the confinement potential [28]—but at $\nu = 2$, the two edge states have opposite spins. As we move beyond $\nu = 2$, we enter the $n = 1$ Landau level. At quarter filling ($\nu = 3$), the valley polarization is arbitrary, but Zeeman coupling favors an aligned spin polarization [13–15]. At half filling ($\nu = 4$), electron correlations can favor either a spin or valley polarized ground state [30], but not both. We label these scenarios I and II, respectively, and show the associated two sequences of edge states in Fig. 2(c). In the following, we call the edge states' spin and valley polarization \uparrow/\downarrow and \pm , respectively.

Figure 3(a) plots g vs ν_T for a fixed $\nu_B = -1$. At low density under the top gate, $g = 0$, whereas around $\nu_T = \nu_B = -1$, $g = 1$. From now on, we report conductance in units of e^2/h and define $g_{\nu_T, \nu_B} = g(\nu_T, \nu_B)$. For $\nu_T = -2$ and -3 , plateaus in conductance occur, although with less quality than for $\nu_T = -1$. To quantify g for $\nu_T = -2$ and -3 , we take an average over the plateau to obtain $g_{\text{exp}} = 0.97 \pm 0.04$ and 0.66 ± 0.005 , where the error is 1σ . A similar plot for $\nu_B = -2$ is shown in Fig. 3(b). Table I lists the expected values of g for full equilibration of edge states (g_{full}) [25], as well as the measured conductances g_{exp} for ν_T up to three. Deviations occur, for example $g_{2,1} \approx 1$ [Fig. 3(a)], instead of $2/3$ as expected for full equilibration, indicating that edge states may not equilibrate.

$g_{2,1} \approx 1$ suggests that the two opposite-spin edge states at $\nu_T = -2$ do not equilibrate on the scale of our device, the \uparrow edge state being fully transmitted through the $\nu_T = -2$ region without scattering. The corresponding $g = 1$ plateau extends at $\nu_B = -1$ from $\nu_T = -1$ to $\nu_T = -2$ with a steep transition occurring only at $\nu_T = -3$ [Fig. 2(a)]. This decrease in g between $\nu_T = -2$ and $\nu_T = -3$ and the existence of well defined plateaus for $g_{3,1}$ and $g_{3,2}$ suggest that the additional \uparrow edge state at $\nu = -3$ does equilibrate. The plasma-etched edges of our samples are highly disordered on the lattice scale, which is expected to induce strong intervalley scattering. Therefore, we assume that the spin polarization is robust, but that edge states with the same spin equilibrate regardless of their valley polarization [along red dashed segments in Table I]. Consequently, we propose a simple model for g closely following Ref. [25], but where only edge states with identical spins equilibrate, regardless of their valley polarization [24]. We use $\nu_{T,\uparrow}(\nu_{T,\downarrow})$ to refer to the number of edge states with spin polarization $\uparrow(\downarrow)$ at filling factor ν_T under the top gate, with similar notations for ν_B . The predicted conductance is then [25]:

$$g_{\text{partial}} = \sum_{i=\downarrow, \uparrow} \frac{\nu_{T,i} \nu_{B,i}}{2\nu_{T,i} - \nu_{B,i}}. \quad (1)$$

At $\nu_T = -3$, only the two edge states polarized spin down would then equilibrate, but not the third with opposite polarization [blue arrow in Table I]. This yields $g_{3,1} = 2/3$ and $g_{3,2} = 5/3$, in excellent agreement with our data, as highlighted in Table I and with dashed black lines on Figs. 3(a)–3(b).

The polarization of the fourth edge state at $\nu_T = -4$ is different for scenarios I and II, allowing us to discriminate between them by measuring the conductance plateaus at $\nu_T = -4$ for different values of ν_B . Using our simple model, we show in Table II the expected conductance

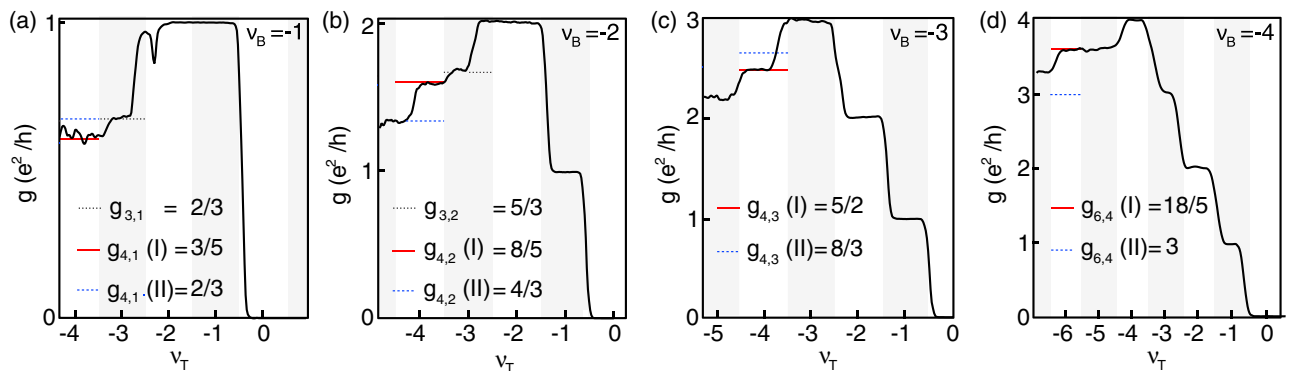


FIG. 3 (color online). Cuts of the two-terminal conductance $g(\nu_T)$ at constant ν_B , measured at 1 K and $B = 14$ T. (a) Cut through $\nu_B = -1$. (b) Cut through $\nu_B = -2$. (c) Cut through $\nu_B = -3$. (d) Cut through $\nu_B = -4$. The conductance plateaus expected from partial edge state equilibration at various values of ν_T are marked by horizontal lines. In some cases, the prediction depends on the polarization of the fourth edge state. In this case, two different scenarios are considered: the fourth edge state is polarized (\uparrow , \downarrow) [Scenario I, red], or (\downarrow , \uparrow) [Scenario II, blue].

TABLE I. Equilibration plateaus for $\nu_{B,T} \leq 3$.

ν_B	ν_T	g_{full}	g_{partial}	g_{exp}	Edge state polarization
1	2	2/3	1	0.98 ± 0.04	
1	3	3/5	2/3	0.66 ± 0.005	
2	3	1.5	5/3	1.68 ± 0.01	

plateaus $g_{\text{partial}}(\text{I})$ and $g_{\text{partial}}(\text{II})$ for the two scenarios, respectively. In scenario I, three \downarrow polarized edge states equilibrate separately from the fourth edge state, which has opposite polarization. This differs from scenario II where there are two edge states of each polarization, and each of those pairs equilibrates separately. For example, Eq. (1) yields $g_{4,3} = 5/2$ for scenario I and $8/3$ for scenario II. In every case, our observed g_{exp} [Table II] accords very well with scenario I (spin-polarized half-filled $n = 1$ level), in agreement with recent transport measurements [30]. In Fig. 3, red and blue lines represent the expected plateaus at $\nu_T = -4$ [panels (a)–(c)] or -6 [panel (d)] for scenarios I and II. The match to data is noticeably better for scenario I. For example, the cut through $\nu_B = -1$ in Fig. 3(a) would not show a transition at $\nu_T = -4$ if the first and fourth edge states at $\nu_T = -4$ did not have the same spin polarization.

In the bipolar regime, nonzero conductance implies disorder-mediated equilibration between edge states at the PN interface [25,31]. Full equilibration would lead to a quantization of the conductance $g = \nu_T \nu_B / (2\nu_T + \nu_B)$, which we do not observe in any of our devices. Even at low field [24], g is not quantized but remains smaller than e^2/h , contrary to what has been observed in more disordered samples. g is strongly suppressed as B increases [Fig. 2], concomitant with the opening of the $\nu = 0$ gap, and reaches on order 10^{-7} S at $B = 14$ T. We attribute this vanishing g to the valley symmetry breaking of the zeroth level. At high fields, our data are consistent with a narrow insulating region ($\nu = 0$ gapped state) spatially separating copropagating p and n edges, suppressing inter-edge state scattering [24].

Similar local gating measurements on GaAs/AlGaAs two dimensional electron gas provided considerable insight into the physics of the integer and fractional quantum Hall

TABLE II. Equilibration plateaus involving $\nu_{B,T} = 4$.

ν_B	ν_T	g_{full}	$g_{\text{partial}}(\text{I})$	$g_{\text{partial}}(\text{II})$	g_{exp}
1	4	4/7	3/5	2/3	0.60 ± 0.03
2	4	4/3	8/5	4/3	1.59 ± 0.005
3	4	12/5	5/2	8/3	2.50 ± 0.002
4	6	3	18/5	3	3.61 ± 0.01

effect, enabling, for example, interferometry [32], equilibration [33], and shot noise [34] measurements. We showed here that comparable studies in graphene and its multilayers are now within reach, with more complex phenomena likely to arise from the additional valley degree of freedom and the ambipolar band structure of graphene.

We thank D. Abanin for his input. This work was funded by the Center for Probing the Nanoscale, an NSF NSEC, supported under Grant No. PHY-0830228. J. R. W. and D. G.-G. acknowledge funding from the W. M. Keck Foundation.

- [1] A. Geim and K. S. Novoselov, *Nat. Mater.* **6**, 183 (2007).
- [2] A. H. Castro-Neto, F. Guinea, N. M. R. Peres, K. S. Novoselov, and A. K. Geim, *Rev. Mod. Phys.* **81**, 109 (2009).
- [3] Y. Zhang, Y.-W. Tan, H. L. Stormer, and P. Kim, *Nature (London)* **438**, 201 (2005).
- [4] K. S. Novoselov, A. K. Geim, S. V. Morozov, D. Jiang, M. I. Katsnelson, I. V. Grigorieva, S. V. Dubonos, and A. A. Firsov, *Nature (London)* **438**, 197 (2005).
- [5] V. P. Gusynin and S. G. Sharapov, *Phys. Rev. Lett.* **95**, 146801 (2005).
- [6] Y. Zhang, Z. Jiang, J. P. Small, M. S. Purewal, Y. W. Tan, M. Fazlollahi, J. D. Chudow, J. A. Jaszczak, H. L. Stormer, and P. Kim, *Phys. Rev. Lett.* **96**, 136806 (2006).
- [7] Z. Jiang, Y. Zhang, H. L. Stormer, and P. Kim, *Phys. Rev. Lett.* **99**, 106802 (2007).
- [8] M. O. Goerbig, *Rev. Mod. Phys.* **83**, 1193 (2011).
- [9] M. Kharitonov, *Phys. Rev. B* **85**, 155439 (2012).
- [10] C. Y. Hou, C. Chamon, and C. Mudry, *Phys. Rev. B* **81**, 075427 (2010).
- [11] Y. Barlas, K. Yang, and A. H. MacDonald, *Nanotechnology* **23**, 052001 (2012).
- [12] J. Alicea and M. P. A. Fisher, *Phys. Rev. B* **74**, 075422 (2006).
- [13] J. Alicea and M. P. A. Fisher, *Solid State Commun.* **143**, 504 (2007).
- [14] L. Sheng, D. N. Sheng, F. D. M. Haldane, and L. Balents, *Phys. Rev. Lett.* **99**, 196802 (2007).
- [15] K. Nomura and A. H. MacDonald, *Phys. Rev. Lett.* **96**, 256602 (2006).
- [16] K. Yang, S. Das Sarma, and A. H. MacDonald, *Phys. Rev. B* **74**, 075423 (2006).
- [17] M. O. Goerbig, R. Moessner, and B. Doucot, *Phys. Rev. B* **74**, 161407 (2006).
- [18] J. Jung and A. H. MacDonald, *Phys. Rev. B* **80**, 235417 (2009).
- [19] J. G. Checkelsky, L. Li, and N. P. Ong, *Phys. Rev. Lett.* **100**, 206801 (2008).
- [20] C. R. Dean, A. Young, I. Meric, C. Lee, L. Wang, S. Sorgenfrei, K. Watanabe, T. Taniguchi, P. Kim, K. Shepard, and J. Hone, *Nat. Nanotechnol.* **5**, 722 (2010).
- [21] F. Amet, J. R. W. Williams, K. Watanabe, T. Taniguchi, and D. Goldhaber-Gordon, *Phys. Rev. Lett.* **110**, 216601 (2013).

- [22] J. Velasco Jr., Y. Lee, L. Jing, G. Liu, W. Bao, and C. N. Lau, *Solid State Commun.* **152**, 1301 (2012).
- [23] R. T. Weitz, M. T. Allen, B. E. Feldman, J. Martin, and A. Yacoby, *Science* **330**, 812 (2010).
- [24] See Supplemental Material at <http://link.aps.org/supplemental/10.1103/PhysRevLett.112.196601> for fabrication details and additional data.
- [25] D. A. Abanin and L. S. Levitov, *Science* **317**, 641 (2007).
- [26] J. R. Williams, L. DiCarlo, and C. M. Marcus, *Science* **317**, 638 (2007).
- [27] B. Ozyilmaz, P. Jarillo-Herrero, D. Efetov, D. A. Abanin, L. S. Levitov, and P. Kim, *Phys. Rev. Lett.* **99**, 166804 (2007).
- [28] D. A. Abanin, P. A. Lee, and L. S. Levitov, *Phys. Rev. Lett.* **96**, 176803 (2006).
- [29] D. A. Abanin, K. S. Novoselov, U. Zeitler, P. A. Lee, A. K. Geim, and L. S. Levitov, *Phys. Rev. Lett.* **98**, 196806 (2007).
- [30] A. F. Young, C. R. Dean, L. Wang, H. Ren, P. Cadden-Zimansky, K. Watanabe, T. Taniguchi, J. Hone, K. L. Shepard, and P. Kim, *Nat. Phys.* **8**, 550 (2012).
- [31] W. Long, Q.-F. Sun, and J. Wang, *Phys. Rev. Lett.* **101**, 166806 (2008).
- [32] C. de C. Chamon, D. E. Freed, S. A. Kivelson, S. L. Sondhi, and X. G. Wen, *Phys. Rev. B* **55**, 2331 (1997).
- [33] G. Muller, D. Weiss, A. V. Khaetskii, K. von Klitzing, S. Koch, H. Nickel, W. Schlapp, and R. Losch, *Phys. Rev. B* **45**, 3932 (1992).
- [34] R. de-Picciotto, M. Reznikov, M. Heiblum, V. Umansky, G. Bunin, and D. Mahalu, *Nature (London)* **389**, 162 (1997).